Recombination Reactions of Atomic Chlorine in Compressed Gases. 2. Geminate and Nongeminate Recombinations and Photolysis Quantum Yields with Argon Pressure Up to 180 bar

T.-T. Song and T.-M. Su*

Department of Chemistry, National Taiwan University, Taipei, Taiwan, R.O.C., and The Institute of the Atomic and Molecular Sciences, Academia Sinica, Taipei, Taiwan, R.O.C.

Received: February 19, 1996; In Final Form: April 23, 1996[⊗]

The laser photolysis/chemiluminescence detection technique was employed to study the recombination reactions of the chlorine atoms generated by photolysis of chlorine molecules with 355 nm laser radiation in compressed Ar gas. The recombination rate constants, the quenching rate constants of the $B\ ^3\Pi(0_u^+)$ and $A\ ^3\Pi(1_u^+)$ states of the chlorine molecules by argon atoms, and the geminate recombination quantum yields were measured over 10−180 bar argon pressure. The recombination quantum yields were found to vary approximately as the third power of the argon density. For the present weak van der Waals system, the low-pressure asymptotic form of the energy relaxation/diffusion model and a simple molecular collision model were employed to account for the density-dependent behavior over the low-to-medium pressure range. The cage effect in the low-pressure regime and its related theoretical models were discussed.

Introduction

For an understanding of the cage effect and its associated molecular dynamics in the condensed phase, the photodissociation and recombination of the halogen molecules, which is generally accepted as a prototype elementary reaction of the kind, has long been intensively studied over a wide range of conditions.[1−29] Among the halogen elements, due to its easier accessibility in the generation and detection methods, iodine has been the most studied molecule.[1−4,6−9,13,15−29] Following-ups were the bromine[10,13,14] and chlorine[5] molecules. Except for the earliest studies,[1,2] in which the photochemical method was employed to follow the reactions, most studies have employed either the flash or laser pump-and-probe technique to monitor the chemical changes.[3−29] With this technique, recently, the time resolution for the probing of the dissociation and recombination of iodine has been pushed to the femtosecond time regime.[24−29]

The chlorine molecule has a well-defined repulsive electronic state C ($^1\Pi_u$) in the near-UV.[30] Its bound electronic states B, A, A', B', and X states have also been characterized.[31−35] As reported in the first part of this study series, the chemiluminescence spectra of the atomic chlorine recombination reactions over 1−175 bar argon pressure have been resolved and assigned.[36] Kinetically, except for the measurement of nongeminate recombination rate constants of chlorine atoms in an earlier study,[5] there were no other related studies in the literature. In this second part of the present work, the time-dependent behavior of the vibrationally resolved chemiluminescence in the chlorine atom recombination reactions was studied by the method of laser photolysis/chemiluminescence detection scheme. The recombination process could be monitored. The nongeminate recombination rate constants, the electronic quenching rate constants, and the geminate recombination quantum yields of chlorine were measured over 10−180 bar argon pressure. On the basis of the experimental results, the cage effect and its corresponding theoretical models in the present pressure regime are discussed.

* To whom correspondence should be addressed at National Taiwan University.

[⊗] Abstract published in *Advance ACS Abstracts,* July 1, 1996.

Kinetic Models

The kinetic models for the geminate and nongeminate recombination reactions of the photodissociated chlorine atoms under argon pressure are analyzed separately in this section. The simplest but yet quite general photodissociation and recombination mechanism for chlorine molecules, which is consistent with the present experimental study, may be written as[37−40]

$$Cl_2 + M \xrightarrow{h\nu} Cl + Cl + M \quad (1)$$

$$Cl + Cl + M \xrightarrow{k_n} Cl_2 + M \quad (2)$$

$$Cl + Cl + M \xrightarrow{k_r} Cl_2^* + M \quad (3)$$

$$Cl_2^* \xrightarrow{k_e} Cl_2 + h\nu \quad (4)$$

$$Cl_2^* + M \xrightarrow{k_q} Cl_2 + M \quad (5)$$

in which M is a third body which may include all the chemical species in the system, Cl_2^* and Cl_2 represent the radiative and nonradiative electronic states of the chlorine molecules, respectively, k_r and k_n are the corresponding recombination rate constants, is the rate constant of photon emission, is the rate constant of the third-body quenching reaction, and eq 1 represents the photodissociation and the simultaneous hot-atom thermalization processes.

Nongeminate Recombination Reaction. In the case that eq 2 represents the nongeminate recombination reaction, for the reaction mechanism of eqs 2−5, the rate equations of [Cl] and [Cl_2^*] are given by

$$d[Cl]/dt = -2(k_r + k_n)[Cl]^2[M] \quad (6)$$

$$d[Cl_2^*]/dt = k_r[Cl]^2[M] - k_e[Cl_2^*] - k_q[Cl_2^*][M] \quad (7)$$

With the initial condition of an instantaneously generated atomic concentration $[Cl]_0$, the time-dependent solutions are

S0022-3654(96)00500-X CCC: $12.00

$$[\mathrm{Cl}]_t = \frac{[\mathrm{Cl}]_0}{1 + 2(k_r + k_n)[\mathrm{M}][\mathrm{Cl}]_0 t} \tag{8}$$

$$[\mathrm{Cl_2}^*]_t = C_1 e^{-k_Q t} \int_0^t \frac{e^{k_Q t'}}{(1 + C_2 t')^2} dt' \tag{9}$$

in which $k_Q = k_e + k_q[\mathrm{M}]$, $C_1 = k_r[\mathrm{Cl}]_0^2[\mathrm{M}]$, $C_2 = 2k_{rec}[\mathrm{M}][\mathrm{Cl}]_0$, and $k_{rec} = k_r + k_n$. The time-dependent photon emission intensity is then proportional to $[\mathrm{Cl_2}^*]_t$.

Long-Time Regime and the Recombination Rate Constants. In the present study we are looking for solutions of eq 9 under experimental conditions such that the atomic chlorine recombination time is much longer than the electronic quenching time. As the time is much longer than $1/k_Q$, the net effect of the quenching process on eqs 2−9 may be approximated by the following transformation. Define the following quenching function as

$$\begin{aligned} f(t - t') &= A_0 e^{-k_Q(t-t')} \qquad t' \le t \\ &= 0 \qquad\qquad\quad t' > t \end{aligned} \tag{10}$$

with

$$A_0 = \frac{k_Q}{1 - e^{-k_Q t}}$$

in which A_0 is the normalization constant. It is obvious that the f function is not an even function, but as $k_Q \to \infty$, the function has all the integration properties of the Dirac δ function. One could symbolically write the following limiting relation:

$$\lim_{k_Q \to \infty} f(t - t') = \delta(t - t')$$

The solution of eq 9 in the long time regime, which describes the time-dependent behavior of the pure recombination reaction, could be obtained in a straightforward way:

$$\begin{aligned} [\mathrm{Cl_2}^*]_t &= \frac{C_1}{k_Q} \int_0^\infty \delta(t - t') \frac{1}{(1 + C_2 t')^2} dt' \\ &= \frac{C_1}{k_Q (1 + C_2 t)^2} \qquad (t > 1/k_Q) \end{aligned} \tag{11}$$

Short-Time Regime and the Quenching Rate Constants of Argon. For the time regime much shorter than the decay time of the recombination, whose time constant is $1/C_2$, one may obtain the following simple approximate solution of eq 9 in the short time domain:

$$[\mathrm{Cl_2}^*]_t = \frac{C_1}{k_Q}(1 - e^{-k_Q t}) \qquad (t \ll 1/C_2) \tag{12}$$

If both the argon and chlorine molecules contribute to the total quenching rate with quenching rate constants k_{q1} and k_{q2}, respectively, then $k_Q = k_e + k_{q1}[\mathrm{Ar}] + k_{q2}[\mathrm{Cl_2}]$. The radiative lifetime of the B state has been measured to be 0.3 ms and that of the A state has been estimated to be 15 ms.[38,41] Since the radiative constants of Cl_2* are much less than the quenching rate under the present experimental conditions, it was neglected in this study. The quenching rate constants of the argon and chlorine molecules could be determined according to this relation.

Geminate Recombination Reaction. If the chlorine atom-pair generated by the photodissociation undergoes the geminate recombination reaction according to eq 2, the rate equations that are consistent with eqs 2−5 become

$$d[\mathrm{Cl}]/dt = -[\mathrm{Cl}]_0 R(t) \tag{13}$$

$$\frac{d[\mathrm{Cl_2}^*]_{gem}}{dt} = -b_r \frac{d[\mathrm{Cl}]}{2\,dt} - k_e[\mathrm{Cl_2}^*] - k_q[\mathrm{Cl_2}^*][\mathrm{M}] \tag{14}$$

in which $[\mathrm{Cl}]_0/2$ is the number density of the geminate atom pairs generated instantaneously, $R(t)$ is the recombination reaction probability rate of the geminate atom pair, and b_r is the branching ratio of the recombination reaction into the radiative electronic states. The solution of $[\mathrm{Cl_2}^*]_{gem}$ may be written as

$$[\mathrm{Cl_2}^*]_{gem,t} = C_0' e^{-k_Q t} \int_0^t e^{-k_Q t'} R(t')\, dt' \tag{15}$$

in which $C_0' = b_r[\mathrm{Cl}]_0/2$. Since in the present study the reaction probability rates of the geminate recombination and the vibrational relaxation rate in the radiative electronic states are, at their longest time scale, in the picosecond time regime, and, on the other end, the quenching rates of the radiative electronic states are in the nanosecond time domain for the fastest cases, the area-normalized function of $R(t')$ could be well approximated by the Dirac δ function, $\delta(0)$. The solution of eq 15 becomes

$$[\mathrm{Cl_2}^*]_{gem,t} = C_0 e^{-k_Q t} \tag{16}$$

in which C_0 is equal to C_0' divided by the normalization constant of $R(t)$.

In the short time regime, the complete time-dependent concentration of Cl_2* could be expressed as the total sum of $[\mathrm{Cl_2}^*]$ generated by the geminate and the nongeminate recombinations:

$$\begin{aligned} [\mathrm{Cl_2}^*]_t^s &= [\mathrm{Cl_2}^*]_t + [\mathrm{Cl_2}^*]_{gem,t} \\ &= \frac{C_1}{k_Q}(1 - C_4 e^{-k_Q t}) \end{aligned} \tag{17}$$

in which $C_4 = 1 - C_0 k_Q / C_1$. Depending on the experimental conditions, C_4 may assume any of the negative, 0, or positive value. At the 0 value, eq 17 is just a step function. As long as the percentage contribution of the geminate recombination is much less than that of the nongeminate recombination, the decoupling of these two processes as implicitly assumed in the form of eq 17 is a good approximation.[42]

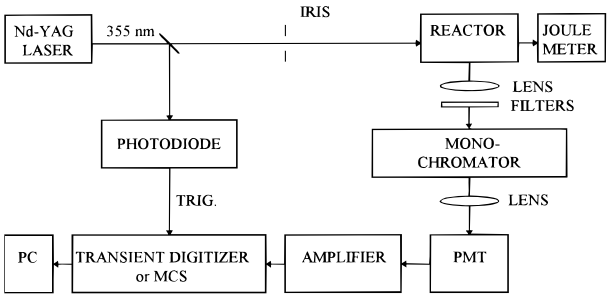

Figure 1. Schematic diagram of the experimental setup. MCS, multichannel scaler; PMT, photomultiplier tube; PC, personal computer.

Experimental Section

Figure 1 shows the schematic diagram of the experimental setup. The basic reaction cell and the chemicals are the same as those reported in the chemiluminescence study.[36] Only the

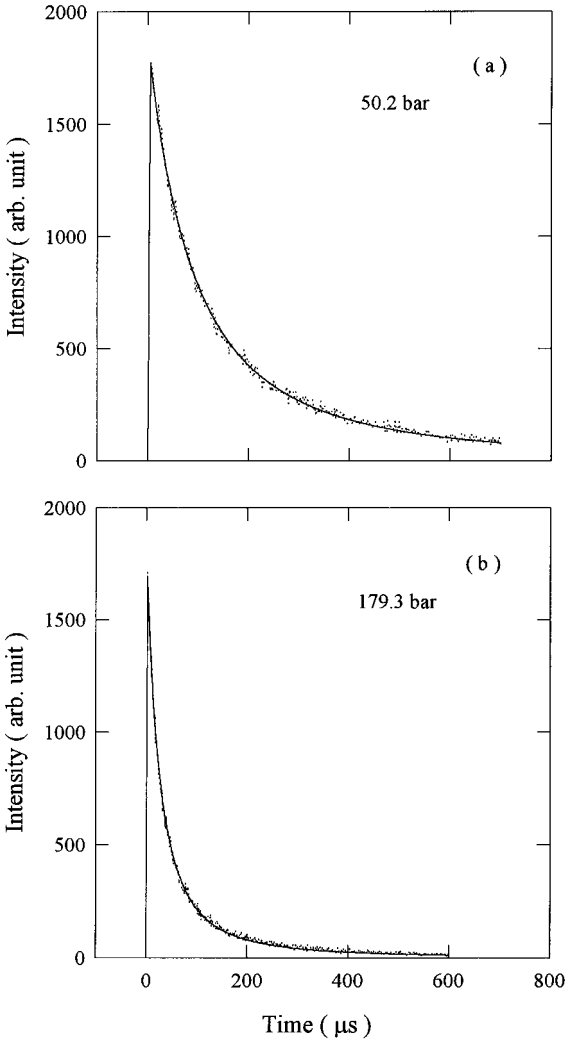

Figure 2. Long-time luminescence decay of the chlorine atom recombination reactions at 50.2 and 179.3 bar argon pressure detected at 843.4 and 844.1 nm, respectively, of the $B(v=0) \rightarrow X(v=11)$ emission. The background noise is less than one unit per channel. The solid lines are the least-squares fitted curves of eq 11.

modifications and the transient photon detection system were briefly described here.

The central portion of the laser beam generated by a Nd:YAG laser operated at 355 nm with a pulse duration of 5 ns was employed to photolyze the chlorine molecules. The laser energy, which was usually controlled in the range 1−3 mJ, was monitored by a calibrated pyroelectric joulemeter. After passing through a set of collecting lenses and a broad-band UV reflection interference filter, the chemiluminescence was dispersed by a 275 mm monochromator (Acton Research) with a reciprocal linear dispersion of 3 nm/mm and then detected by a thermoelectrically cooled red-enhanced photomultiplier tube (Hamamatsu, R943-02). Usually a slit width of 1.0 mm was used. Since the laser spatial profile was close to a top-hat shape, and assuming that the photon absorption follows Beer's law, the average chlorine atom concentrations in the center position of the reactor could be determined by the average laser energy absorbed by the chlorine molecules. For the recombination rate measurements, in which the chemiluminescence signals may last up to hundreds of microseconds, a multichannel scaler (Canberra) with a dwell time of either 0.5 or 0.2 μs was used for the signal accumulation. For the fast quenching process, a transient digitizer (Gould-Biomation) with a sampling time of 5 ns was employed. All the data were then stored and simulated by a personal computer. In most of the present experimental runs, the chlorine pressure was kept at 5.33 mbar and the argon pressure was varied from 10 to 180 bar. The reactor was kept at 300 K by a thermostat.

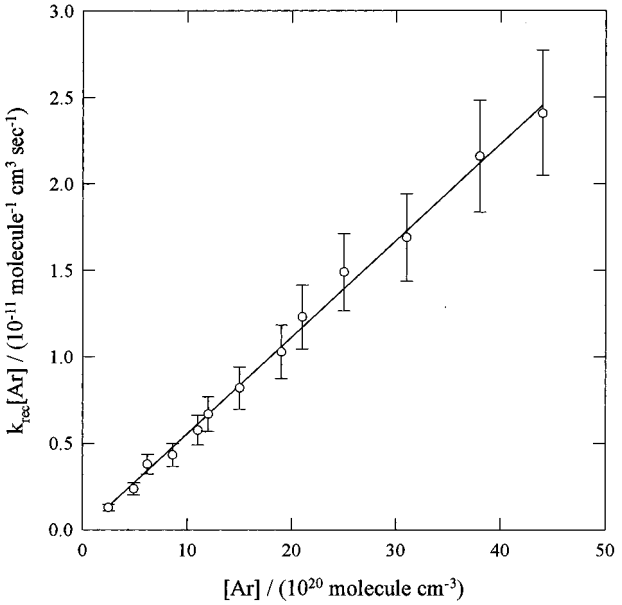

Figure 3. Measured k_{rec}[Ar] as a function of the Ar density. The solid line is the least-squares fitting of a linear function.

TABLE 1: Recombination Rate Constants of Chlorine Atoms in Ar

$k_{rec}/10^{-32}$ cm^6 molecule^{-2} s^{-1}	pressure/bar	methods	ref
0.55 ± 0.08 (300 K)	10−173	*a*	this work
1.13 ± 0.23 (296 K)	0.6−1.7	*a*	40
1.10 (313 K)	<0.004	*b*	43
1.17 ± 0.22 (293 K)	<0.003	*c*	44
1.21 ± 0.14 (298 K)	<0.003	*c*	45
1.46 ± 0.09 (293 K)	~0.33	*d*	46
2.04 ± 0.83 (298 K)	0.5−24	*d*	5

[a] Laser photolysis/chemiluminescence detection. [b] Discharge flow/isothermal calorimetric atom detection. [c] Discharge flow/chemiluminescence detection. [d] Flash photolysis/Cl_2 transient absorption detection.

Results and Discussion

Nongeminate Recombination Rate Constants. Figure 2 shows the typical recombination chemiluminescence signals in the long-time regime at 50.2 and 179.3 bar argon pressure, respectively. In this time domain the reaction is essentially due to the recombination of nongeminate chlorine atom-pairs. The emission of $B(v=0) \rightarrow X(v=11)$ vibrational band, whose maximum intensity appears at wavelength 843.4 nm under 50.2 bar and 844.1 nm under 179.3 bar argon pressure, was monitored. The average chlorine atom concentrations were determined to be 4.12×10^{14} and 4.02×10^{14} molecules cm^{-3} at these two pressures, respectively.

The time-dependent decay curves were fitted with eq 11 and also shown in the figure. The constants k_{rec}[Ar] in the argon pressure range 10−173 bar were determined and are shown in Figure 3. The error bars, which were estimated to be about 15%, were mainly coming from the uncertainties in determining the chlorine atom concentrations. These uncertainties mainly originated from errors in the measurements of the laser energy and the laser spatial size. A linear least-squares fitting could be obtained and the average recombination constant over the whole pressure range was determined to be $(0.55 \pm 0.08) \times 10^{-32}$ cm^6 molecule^{-2} s^{-1}. As listed in Table 1, the recombination rate constant is in reasonably good agreement with the

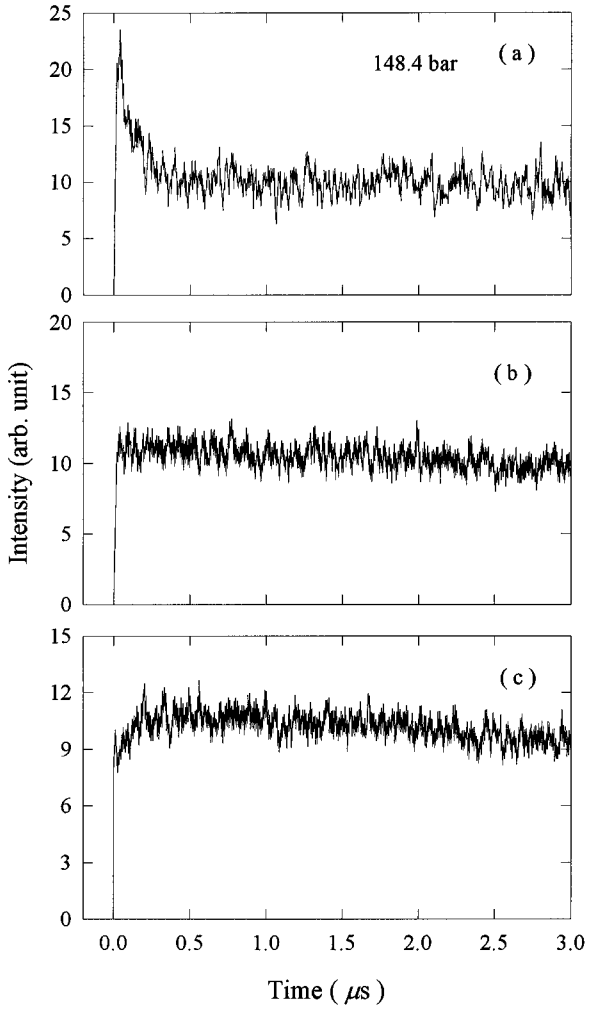

Figure 4. Transient luminescence intensity of chlorine atom recombination under 148.4 bar argon pressure detected at the wavelength 844.1 nm ($B(v=0) \rightarrow X(v=11)$). From (a) to (c), the chlorine atom concentrations are 2.75, 4.67, and 9.37×10^{14} molecule cm^{-3}, respectively.

results measured at lower argon pressure with completely different preparation and detection techniques.[5,40,43−46] This suggests that the diffusion-controlled recombination process has not yet contributed to the total recombination rate up to 180 bar argon pressure.

Geminate Recombination and the Quenching Rate Constants of Argon. As shown by eq 17, if the chlorine atoms follow the proposed mechanism, one should be able to observe the short-time behavior of the chemiluminescence intensity varying from a rising trend to a step function and finally switching to a decaying type of the signal as the initial chlorine atom concentration varying from a high to a low value. Figure 4 shows the time-dependent luminescence intensities detected at 844.1 nm as the initial chlorine atom concentrations were at 2.75, 4.67, and 9.37×10^{14} molecules cm^{-3}, respectively, and the argon pressure was kept at 148.4 bar. The background noise was close to 0. The slow long-time decay slope at the higher chlorine atom concentrations was due to the atomic recombination. The experimental observations are in excellent agreement with the model predictions. The short-time luminescence intensities were fitted with eq 17 over the pressure range 25.5−179.3 bar. Figure 5 shows two typical fittings at 75.0 and 179.3 bar argon pressure, respectively. The corresponding total quenching rates k_Q were listed in Table 2 and also shown in Figure 6. Apparently, within the experimental uncertainty, the quenching rate constants were slightly increased in the high-

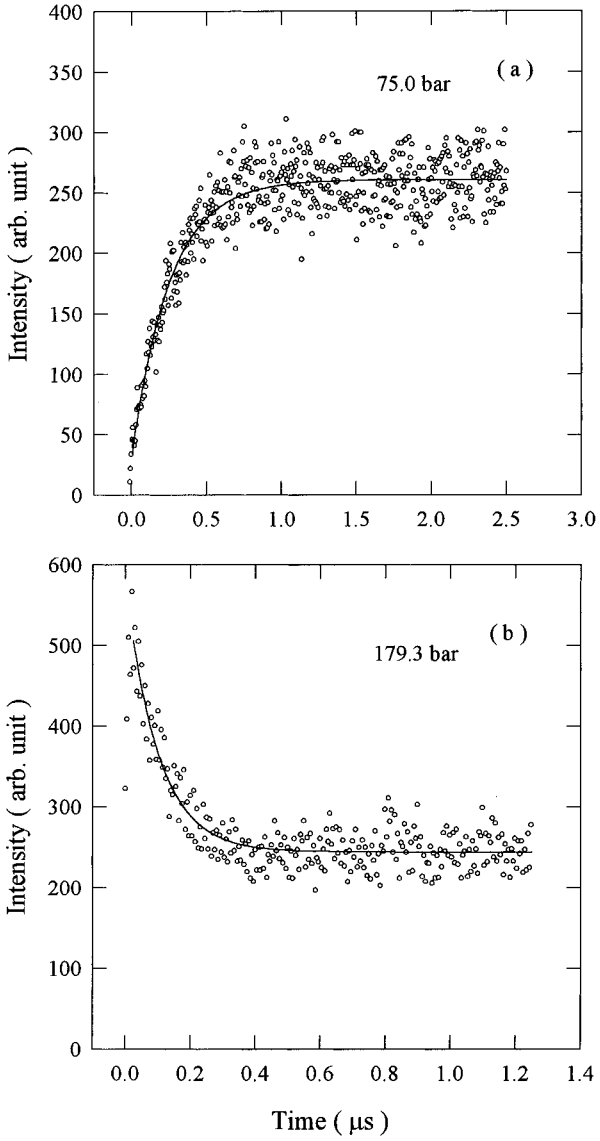

Figure 5. Transient luminescence intensity detected at 843.8 and 844.1 nm ($B(v=0) \rightarrow X(v=11)$) under 75.0 and 179.3 bar argon pressures, respectively. The background noise is less than one unit per channel. The solid lines are the least-squares fittings of eq 17.

TABLE 2: Total Quenching Rate Constants and the Geminate Recombination Quantum Yields for Chlorine Photolysis at 355 nm in Ar

P(Ar)/bar	[Ar]/(10^{21} molecules cm^{-3})	k_Q /(10^6 s^{-1})	recombination yield (%)
25.5	0.62	1.79 ± 0.06	0.005
50.2	1.25	3.10 ± 0.13	0.019
74.9	1.88	3.97 ± 0.16	0.027
99.9	2.52	5.44 ± 0.41	0.076
125.0	3.14	7.01 ± 0.63	0.103
129.8	3.30	7.05 ± 0.81	0.167
140.6	3.56	8.55 ± 1.58	0.236
149.0	3.79	8.80 ± 0.67	0.346
160.3	4.06	9.17 ± 0.58	0.375
179.3	4.56	10.0 ± 0.62	0.504

pressure regime. The asymptotic low-pressure quenching rate could be approximated as $k_Q = k_{q1}[Ar] + k_{q2}[Cl_2]$. From the slope, one obtained the low-pressure (0−100 bar) quenching rate constant of Ar at 300 K to be $(1.87 \pm 0.12) \times 10^{-15}$ $molecule^{-1}$ cm^3 s^{-1}. From the intercept of Figure 6 and the chlorine pressure 5.33 mbar, one obtained the quenching rate constant by the chlorine molecules to be 5.0×10^{-12} $molecule^{-1}$ cm^3 s^{-1}, a value in good agreement with the reported quenching

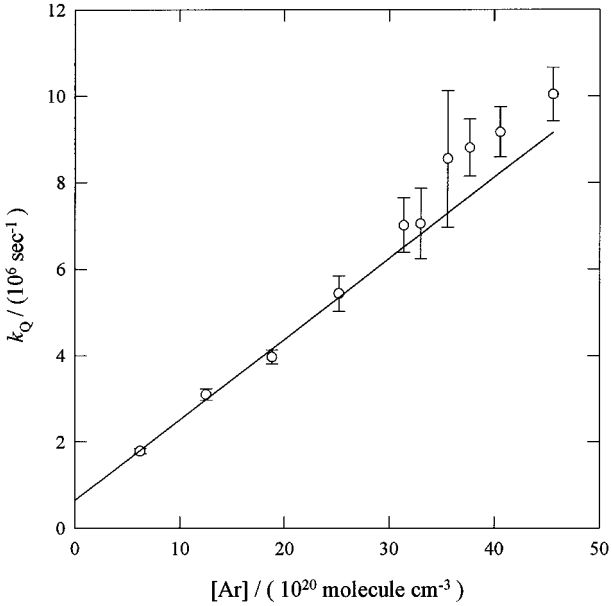

Figure 6. Total quenching rate k_Q as a function of the argon density. The solid line is the low-pressure asymptotic linear least-squares fitted curve below 100 bar. The intercept value is corresponding to the quenching rate of the chlorine molecules in the experiments.

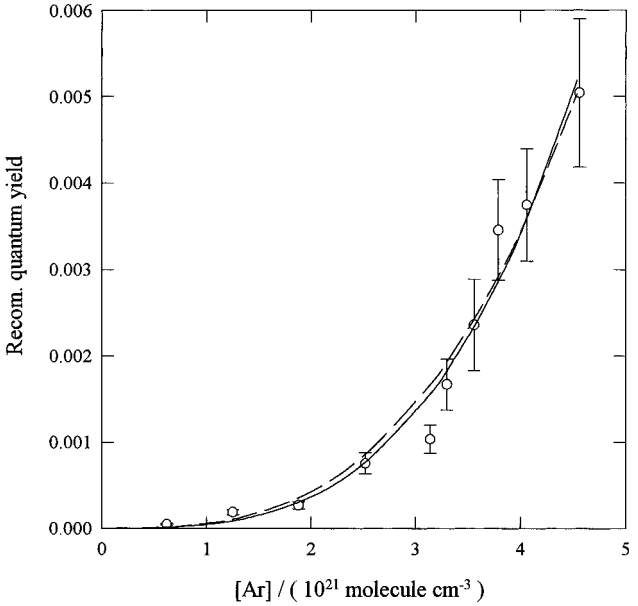

Figure 7. Geminate recombination quantum yield of chlorine molecules at 355 nm radiation as a function of the argon density. The solid curve is the least-squares fitting of eq 18, and the dashed curve is the least-squares fitting of the cubic density term only.

rate constant $(6.4 \pm 0.2) \times 10^{-12}$ molecule^{-1} cm^3 s^{-1} measured in the millibar chlorine pressure regime.[38] The quenching rate constants of argon were not available in the literature for comparison.

The quenching rates were also measured at the higher vibrational emission band $B(v=1) \rightarrow X(v=11)$ under 50.2, 99.9, and 179.3 bar argon pressures. Within the experimental uncertainties, the rates measured were the same as those obtained from the (0,11) band. Under the same conditions, the quenching rates measured from the emission of $A \rightarrow X$ are also equal to those obtained at the $B \rightarrow X$ emissions within the experimental uncertainties. All these observations suggest that the inter-electronic state crossing among the closely spaced excited electronic states, which may include A, A', B, and B' states, and the vibrational energy relaxation within these states are all faster than the electronic quenching rate. The measured electronic quenching rates were just the net transfer rates from these excited states to the X state under the present experimental conditions. These observations are consistent with the previous steady-state chemiluminescence study in which the Boltzmann population distribution was observed over the B and A electronic states under the present experimental conditions.[36]

Geminate Recombination Quantum Yields of Chlorine at 355 nm Radiation and the Cage Effect in the Low Argon Pressure Regime. Since the chlorine atoms generated by 355 nm eventually recombined with each other back to the chlorine molecules, the chemiluminescence signals measured are directly proportional to the number density of the chlorine atom pairs recombined, either in the geminate or in the nongeminate forms. One may decompose the time-dependent chemiluminescence signals into the geminate and the nongeminate parts and then obtain their individual total emissions by integrating over the time of the recombination. Under the present experimental conditions, geminate recombination accounts at most for a mere 0.5% of the total recombinations. One may approximate the total chlorine atom pairs generated by 355 nm by the nongeminate recombination. The geminate recombination quantum yields for chlorine photolysis are then just the ratio between the geminate and nongeminate recombination chemiluminescence signals.

Figure 7 shows the geminate recombination quantum yields of chlorine photolysis over the argon pressure 26−179 bar. The corresponding quantities are listed in Table 2. It varies from a very low 0.005% at 25.5 bar to an appreciable 0.504% at 179.3 bar. The variation of the recombination quantum yield as a function of the argon density could be fitted with either a simple cubic or the following cubic plus quartic terms:

$$\varphi_{rec} = a[\mathrm{Ar}]^3 + b[\mathrm{Ar}]^4 \qquad (18)$$

No other pressure-dependent terms were found to be significant for this pressure range. For the simple cubic relation, the least-squares fitted a is $(5.37 \pm 0.21) \times 10^{-5}$ (10^{21} molecules cm^{-3})$^{-3}$, and for eq 18, a and b are $(3.88 \pm 1.09) \times 10^{-5}$ (10^{21} molecules cm^{-3})$^{-3}$ and $(3.66 \pm 4.12) \times 10^{-6}$ (10^{21} molecules cm^{-3})$^{-4}$, respectively. As shown in Figure 7, the experimental data could be fitted reasonably well by either one of the two relations. Nevertheless, a closer comparison reveals that the fitting of eq 18 is slightly better than that of the simple cubic relation. Despite their differences, both relations reveal that the cubic density variation is the dominant term. If the cluster mechanism were responsible for the above geminate recombination, one would need to postulate that recombinations come from the dissociation of the Ar_3Cl_2 and Ar_4Cl_2 clusters to account for the cubic and quartic variations of the argon pressure. However, molecular dynamics study at 180 bar argon pressure showed that the recombinations mainly come from the secondary geminate recombination, i.e., most of the recombining chlorine atoms have traveled beyond the first average argon shell before they come back to each other again.[47] Also, if the cluster mechanism should be the case, there are no compelling reasons to discard the possible contributions of the smaller size clusters, such as $ArCl_2$ and Ar_2Cl_2, which are bound to be more bountiful than the higher clusters in the present experiments.

One simple model which could account for the cubic pressure behavior over the present pressure range is the energy relaxation/diffusion model proposed by Troe and co-workers.[6,9,10,13] The recombination quantum yield was expressed as

$$\varphi_{rec} = \frac{R}{r_0}\left\{\frac{k_{rec}^{g}}{k_{rec}^{g} + 4\pi RD}\right\} \qquad (19)$$

in which R is the contact distance of the chlorine atom pair in the diffusion equation, r_0 is the most probable separation distance of the chlorine atom pair in the photodissociation, k_{rec}^g is the value of the recombination rate coefficient in the absence of diffusion control and in the present case is equal to the experimental k_{rec}[Ar] values, and D is the mutual diffusion coefficients of the chlorine atom-pair in argon. Here, k_{rec}^g is measured in molecular units. Applying this equation to the present low-pressure regime, one obtains the following pressure relations:

$$k_{rec}^g \rightarrow k_{rec}[\mathrm{Ar}] \propto [\mathrm{Ar}] \tag{20}$$

$$r_0 \propto [\mathrm{Ar}]^{-1} \tag{21}$$

$$D \propto [\mathrm{Ar}]^{-1} \tag{22}$$

$$4\pi RD \gg k_{rec}^g \tag{23}$$

Substituting eqs 20−23 into eq 19, one finds that the recombination quantum yield is directly proportional to the cube of the argon density. Obviously, the low-pressure asymptotic form of the energy relaxation/diffusion model is consistent with the present main feature of the experimental observation. Nevertheless, one has to be cautious of the physical interpretation of the equation. The major point is that in this comparatively low-pressure regime, the mean free path of the chlorine atoms is already much longer than the dimension of the boundary condition of the diffusion equation which may invalidate the applicability of the results obtained under high-pressure or high-density conditions. Another point is that the above equation could not account for the quartic variation of the quantum yield, even though it appears to be as a secondary contribution.

A simplified molecular collision model which is also capable of modeling the present density-dependent behavior of the quantum yield is proposed as follows:

$$\mathrm{Cl_2} + \mathrm{M} \xrightarrow{h\nu} \mathrm{Cl}(\mathbf{r}_1) + \mathrm{Cl}(\mathbf{r}_2) + \mathrm{M} \tag{24}$$

$$\mathrm{Cl}(\mathbf{r}_1) + \mathrm{M} \leftrightarrow \mathrm{MCl}(\mathbf{r}_1) \quad \text{(or higher clusters)} \tag{25}$$

$$\mathrm{Cl}(\mathbf{r}_2) + \mathrm{MCl}(\mathbf{r}_1) \rightarrow \mathrm{Cl_2} + \mathrm{M} \tag{26}$$

in which the first reaction emphasizes the hot atom thermalization with two chlorine atoms being separated by $r_0 = |\mathbf{r}_1 - \mathbf{r}_2|$, the second reaction represents the formation of the chlorine atom clusters, and the third reaction is the formation of the stable Cl_2 by direct molecular collision instead of the diffusion motion. In the low enough pressure regime, the value of r_0 is directly proportional to the mean collision distance between the chlorine and Ar atoms and, therefore, is inversely proportional to the argon density. In the final recombining step, the reaction does not proceed through diffusion; rather it occurs approximately by the molecular kinetic collision motion in the low-pressure regime. The reaction probability of reaction 26 would then be proportional to the solid angle of the chlorine cluster with respect to the chlorine atom, which is inversely proportional to the square of r_0 and also to the concentration of ArCl. Taking these two factors together, the geminate recombination probability would be proportional to the third power of the argon density if the ArCl clusters were involved and to the fourth power if Ar_2Cl clusters took part in the reaction. One may note that the present model could be regarded as an extension of the conventional bound-complex mechanism for the nongeminate recombination reactions in low-pressure gases. The recombination quantum yields could be calculated either by the phenomenological eq 19 or by the molecular dynamics method. Both methods were attempted at 180 bar argon pressure. First, the molecular dynamics was employed to simulate the photodissociation and recombination of the chlorine molecules into the four bound electronic states X, A', A, and B'. Since the present experiment was carried out at constant temperature instead of constant energy condition, and also the recombination rate constants are sensitive to the temperature, to simulate the present experiment, the most natural choice of statistical ensemble would be the NVT ensemble. The Nose−Hoover molecular dynamics,[48−50] which gives a canonical ensemble, was employed in the present calculations. With a system composed of 106 argon atoms and one chlorine molecule, the trajectories of the chlorine atom-pair were followed up to 400 ps after the absorption of a 355 nm photon by initially switching the potential from the ground state to the repulsive C state and then switching to one of the above four bound potentials as their potential difference being less than $^1/_2kT$ during the dissociation process. A total of around 8000 trajectories was calculated for each potential. The recombination events were recorded. The calculated recombination quantum yields of the above four bound states are 0.039, 0.023, 0.019, and 0.014, respectively, if each single recombination channel was considered independently.[47] Under the present relatively low-density conditions, a preferential transfer of population among the electronic states involved in the recombination process is expected to be not important during the recombination stage. Taking into account the electronic degeneracy factors $^1/_{16}$, $^2/_{16}$, $^2/_{16}$, and $^1/_{16}$, for the above states, respectively, one obtained a total recombination quantum yield of 0.86%. Compared with the present experimental value of 0.50%, the agreement is good.

In the case of eq 19, at 180 bar argon, $k_{rec}^g = 2.51 \times 10^{-11}$ cm^3 molecule^{-1} sec^{-1}, $R = 3.58$ Å, $r_0 = 36.9$ Å, and $D = 2.14 \times 10^{-3}$ cm^2 s^{-1}, the equation would yield a recombination quantum yield of 0.24%. In these calculations, the R value was set at the chlorine atom-pair internuclear distance as the X state potential being $2kT$ below the dissociation limit; r_0 was identified as the most probable internuclear distance as the hot chlorine atoms being thermalized to within $^1/_2kT$ of the average thermal energy at 355 nm radiation and was calculated by the molecular dynamics method;[47] D was calculated according to the procedure of Troe et al.[9,10,13] The electronic degeneracies of the states involved in the recombination were already implicitly included in the equation. Obviously, the prediction of the phenomenological equation 0.24% is in good agreement with the measured result 0.50%. Finally, as a reminder, for the results calculated by the molecular dynamics method, only the interaction potentials determined by the spectroscopic methods were needed. However, in obtaining the values of the phenomenological equation, both the measured recombination rate constants and the chlorine atom-pair internuclear separation due to the hot atom thermalization process were needed. The latter quantity was usually not easily amenable to the experiments under the present low-to-medium pressure conditions.

In summary, for cases of weak interaction systems with the photodissociation energy well above the dissociation energy, i.e., the excess energy is much larger than the thermal energy, such as the present Cl_2/Ar system and experimental condition, the above molecular collision model may be applied. The geminate recombination in the low-to-medium pressure regime is mainly due to the spatial confinement of the recombining particles by the buffer gas. The whole process is simply governed by the laws of the gas kinetics. In other words, the cage effect known in the condensed phase is still operating in

the present low-to-medium pressure range. However, there is still a subtle difference between them: in the present case, the cage is a loose kind instead of the tight type as revealed in the higher pressure regime or in the condensed phase. For systems with stronger van der Waals forces and/or the photon energy being close to the dissociation energy of the molecules, or systems with both the dissociation and recombination processes being proceeded in the same electronic state, the cluster model as proposed by Troe and co-workers may become the dominant mechanism for the quantum yields in the low pressure regime, as demonstrated in the I_2/CO_2, I_2/C_2H_4, and Br_2/CO_2 systems.[9,10,13]

Conclusions

The recombination rate constants, the quenching rate constants of the *A* and *B* states of the chlorine molecules by argon atoms and the geminate recombination quantum yields of the chlorine atom pairs were measured by the laser photolysis/chemiluminescence detection scheme over the argon pressure 10−180 bar. The recombination quantum yields could be quantitatively calculated by both the low-pressure asymptotic form of the energy relaxation/diffusion model and the methods of molecular dynamics. The agreement between the theoretical and experimental results is very good. This suggests that under the present experimental conditions and because of the relatively weak van der Waals interactions of the system, the cage effect was due to the spatial confinement of the chlorine atom pairs according to the laws of gas kinetics. Nevertheless, in the other situations, such as the clusters in the supersonic molecular beam experiments or the molecular systems with strong van der Waals force in the low-to-medium pressure buffer molecules, the cluster model could be the dominant mechanism for the photolytic cage effect. It is quite possible that under some specially designed conditions, these two mechanisms might operate with similar importance.

Acknowledgment. T.M.S. wishes to thank Prof. J. Troe of Göttingen University for illuminating discussions and helpful suggestions. The financial support by the National Science Council, Republic of China, is gratefully acknowledged.

References and Notes

(1) Franck, J.; Rabinovitch, E. *Trans. Faraday Soc.* **1934**, *30*, 120.
(2) Lampe, F. W.; Noyes, R. M. *J. Am. Chem. Soc.* **1954**, *76*, 2140.
(3) Luther, K.; Troe, J. *Chem. Phys. Lett.* **1974**, *24*, 85.
(4) Chuang, T. J.; Hoffman, G. W.; Eisenthal, K. B. *Chem. Phys. Lett.* **1974**, *25*, 201.
(5) Hippler, H.; Troe, J. *Int. J. Chem. Kinet.* **1976**, *8*, 501.
(6) Luther, K.; Schroeder, J.; Troe, J.; Unterberg, U. *J. Phys. Chem.* **1980**, *84*, 3072.
(7) Dutoit, J. C.; Zellweger, J. M.; van den Beger, H. *J. Chem. Phys.* **1983**, *78*, 1825.
(8) Bado, P.; Wilson, K. R. *J. Phys. Chem.* **1984**, *88*, 655.
(9) Otto, B.; Schroeder, J.; Troe, J. *J. Chem. Phys.* **1984**, *81*, 202.
(10) Hippler, H.; Schubert, V.; Troe, J. *J. Chem. Phys.* **1984**, *81*, 3931.
(11) Kelley, D. F.; Abul-Haj, N. A.; Jang, D.-J. *J. Chem. Phys.* **1984**, *80*, 4105.
(12) Bado, P.; Dupuy, C.; Magda, D.; Wilson, K. R. *J. Chem. Phys.* **1984**, *80*, 5531.
(13) Hippler, H.; Otto, B.; Schroeder, J.; Schubert, V.; Troe, J. *Ber. Bunsen-Ges. Phys. Chem.* **1985**, *89*, 240.
(14) Abul-Haj, N. A.; Kelley, D. F. *Chem. Phys. Lett.* **1985**, *119*, 182.
(15) Berg, M.; Harris, A. L.; Harris, C. B. *Phys. Rev. Lett.* **1985**, *54*, 951.
(16) Harris, A. L.; Berg, M.; Harris, C. B. *J. Chem. Phys.* **1986**, *84*, 788.
(17) Abul-Haj, N. A.; Kelley, D. F. *J. Chem. Phys.* **1986**, *84*, 1335
(18) Smith, D. E.; Harris, C. B. *J. Chem. Phys.* **1987**, *87*, 2709.
(19) Schroeder, J.; Troe, J. *Annu. Rev. Phys. Chem.* **1987**, *38*, 163.
(20) Harris, A. L.; Brown, J. K.; Harris, C. B. *Annu. Rev. Phys. Chem.* **1988**, *39*, 341.
(21) Xu, X.; Lingle, R. Jr.; Yu, S.-C.; Zhu, H.; Hopkins, J. B. *J. Chem. Phys.* **1990**, *93*, 5667.
(22) Xu, X.; Yu, S.-C.; Lingle, R. Jr.; Zhu, H.; Hopkins, J. B. *J. Chem. Phys.* **1991**, *95*, 2445.
(23) Fei, S.; Zheng, X.; Heaven, M. C.; Tellinghuisen, J. *J. Chem. Phys.* **1992**, *97*, 6057.
(24) Liu, Q.; Wang, J.-K.; Zewail, A. H. *Nature* **1993**, *364*, 427.
(25) Lienau, Ch.; Williamson, J. C.; Zewail, A. H. *Chem. Phys. Lett.* **1993**, *213*, 289.
(26) Lienau, Ch.; Zewail, A. H. *Chem. Phys. Lett.* **1994**, *222*, 224.
(27) Zadoyan, R.; Li, Z.; Martens, C. C.; Apkarian, V. A. *J. Chem. Phys.* **1994**, *101*, 6648.
(28) Lienau, Ch.; Zewail, A. H. *J. Chim. Phys.* **1995**, *92*, 566.
(29) Wang, J.-K.; Liu, Q.; Zewail, A. H. *J. Phys. Chem.* **1995**, *99*, 11309.
(30) Brith, M.; Rowe, M. D.; Schnepp, O.; Stephens, P. J. *Chem. Phys.* **1975**, *9*, 57.
(31) Coxon, J. A. *J. Mol. Spectrosc.* **1980**, *82*, 264.
(32) Ishiwata, T.; Ishiguro, A.; Obi, K. *J. Mol. Spectrosc.* **1991,** *147*, 300.
(33) Tellinghuisen, P. C.; Guo, B.; Chakraborty, D. K.; Tellinghuisen, J. J. *Mol. Spectrosc.* **1988**, *128*, 268.
(34) Ishiwata, T.; Kasai, Y.; Obi, K. *J. Chem. Phys.* **1991**, *95*, 60.
(35) Douglas, A. E.; Hoy, A. R. *Can. J. Phys.* **1975**, *53*, 1965.
(36) Chang, L.-C.; Song, T.-T, Tai, C.-C.; Su, T.-M. *J. Phys. Chem.*, submitted.
(37) Clyne, M. A. A.; Smith, D. J. *J. Chem. Soc., Faraday Trans. 2* **1979**, *75* 704.
(38) Clyne, M. A. A.; Martinez, E. *J. Chem. Soc., Faraday Trans. 2* **1980**, *76*, 1275.
(39) Hwang, C.-J.; Jiang, R.-C.; Su, T.-M. *J. Chem. Phys.* **1986**, *84*, 5095.
(40) Weng, C.-J.; Ho, T.-I.; Su, T.-M. *J. Phys. Chem.* **1987**, *91*, 5237.
(41) Coxon, J. A. *Molecular Spectroscopy*; Barrow, R. F., Long, D. A., Millen, D. J., Eds.; Specialist Periodical Reports, The Chemical Society: London, 1972; Vol. 1, Chapter 4.
(42) Jung, Y.; Lee, S. *Chem. Phys. Lett.* **1994**, *231*, 429.
(43) Bader, L. W.; Ogryzlo, E. A. *Nature (London)* **1964**, *201*, 491.
(44) Hutton, E.; Wright, M. W. *Trans. Faraday Soc.* **1965**, *61*, 78.
(45) Clyne, M. A. A.; Stedman, D. H. *Trans. Faraday Soc.* **1968**, *64*, 2698.
(46) Widman, R. P.; DeGraff, B. A. *J. Phys. Chem.* **1973**, *77*, 1325.
(47) Song, T.-T.; Hwang, Y. S.; Su, T.-M., to be published.
(48) Nose, S. *J. Chem. Phys.* **1984**, *81*, 511.
(49) Nose, S. *Mol. Phys.* **1984**, *52*, 255.
(50) Hoover, W. G. *Phys. Rev.* **1985**, *A31*, 1695.

JP9605008